Sparseness Constrained Nonnegative Matrix Factorization for Unsupervised 3D Segmentation of Multichannel Images: Demonstration on Multispectral Magnetic Resonance Image of the Brain

Ivica Kopriva[1*], Ante Jukić[1] and Xinjian Chen[2]

[1]Division of Laser and Atomic Research and Development, Ruđer Bošković Institute, Bijenička cesta 54, P.O. Box 180, 10002, Zagreb, Croatia

[2]School of Electronics and Information Engineering, Soochow University, Suzhou City, 215006, China
e-mail: ikopriva@irb.hr, Ante.Jukic@irb.hr, myfuturejian@gmail.com

Abstract

A method is proposed for unsupervised 3D (volume) segmentation of registered multichannel medical images. To this end, multichannel image is treated as 4D tensor represented by a multilinear mixture model, i.e. the image is modeled as weighted linear combination of 3D intensity distributions of organs (tissues) present in the image. Interpretation of this model suggests that 3D segmentation of organs (tissues) can be implemented through sparseness constrained factorization of the nonnegative matrix obtained by mode-4 unfolding of the 4D image tensor. Sparseness constraint implies that only one organ (tissue) is dominantly present at each pixel or voxel element. The method is preliminary validated, in term of Dice's coefficient, on extraction of brain tumor from synthetic multispectral magnetic resonance image obtained from the TumorSim database.

Keywords: Multispectral magnetic resonance image, brain tumor delineation, unsupervised segmentation, sparseness, nonnegative matrix factorization.

1 INTRODUCTION

The purpose of this paper is development of sparseness constrained nonnegative matrix factorization (NMF) method for unsupervised (a.k.a. blind or automatic) 3D (volume) segmentation of registered multichannel medical images. That is in contrast to existing matrix or tensor factorization based methods that perform unsupervised segmentation of the multichannel image on a slice-by-slice basis, [1, 2]. Proposed 3D segmentation approach is expected to improve accuracy when compared against slice-by-slice approach. That is explained by multilinear mixture model (mLMM) of the multi-sliced multichannel 4D image tensor where mode-4 matrix stands for what in blind source separation (BSS) is known as a mixing matrix, [3, 4], and that is the same for all the slices. As opposed to that, in bilinear mixture model (bLMM), that is characteristic for slice-by-slice approach to image segmentation, mixing matrix is slice dependent. Here, we propose a novel approach to 3D segmentation through sparseness constrained factorization of nonnegative matrix obtained by mode-4 unfolding of the multi-slice multichannel image tensor. Sparseness constraint is necessary to ensure uniqueness of related matrix factorization problem i.e. to limit, otherwise infinite, number of indeterminacies characteristic for BSS to permutation and scaling indeterminacies only. Sparseness constraint implies that only small

* ikopriva@irb.hr, phone: +385 1 4571 286; fax: +385 1 4680 104; http://www.lair.irb.hr/ikopriva/.

number (possibly even one) of the overall number of organs (tissues) in the image is dominantly present at each pixel or voxel element. While proposed method is demonstrated herein on segmentation of brain tumor from 21 slices of synthetic multispectral magnetic resonance (mMR) image downloaded from the TumorSim database, [5], its applicability is more general. That is, the method can be applied to 3D segmentation of organs (tissues) from registered multichannel images acquired in other medical imaging modalities. Few examples include multi-phase computed tomography (CT), diffusion tensor, multispectral/hyperspectral and/or optical coherence tomography images.

2 MATERIALS AND METHODS

For the purpose of unsupervised 3D segmentation registered multichannel image is represented in a form of the mLMM:

$$\underline{\mathbf{X}} \approx \underline{\mathbf{G}} \times_1 \mathbf{A}^{(1)} \times_2 \mathbf{A}^{(2)} \times_3 \mathbf{A}^{(3)} \times_4 \mathbf{A}^{(4)} \tag{1}$$

where $\underline{\mathbf{X}} \in \mathbb{R}_{0^+}^{I_1 \times I_2 \times I_3 \times I_4}$ represents multichannel image consisting of I_4 channel images, I_3 slices and $I_1 \times I_2$ pixel (voxel) elements per slice, i.e. multichannel image is 4D tensor. $\mathbb{R}_{0+}$ is a real manifold with nonnegative elements. mLMM in (1) is also known as Tucker4 model, [6, 7], where $\underline{\mathbf{G}} \in \mathbb{R}_{0+}^{J_1 \times J_2 \times J_3 \times J_4}$ is known as core tensor, $\left\{ \mathbf{A}^{(n)} \in \mathbb{R}_{0^+}^{I_n \times J_n} \right\}_{n=1}^{4}$ are factor matrices and $\times_n$ denotes *n*-mode product of a tensor with a matrix $\mathbf{A}^{(n)}$. In model (1) factor matrices associated with the first three modes represent directional bases along first three dimensions of tensor $\underline{\mathbf{X}}$. Hence, they can be used to model a source tensor:

$$\underline{\mathbf{S}} = \underline{\mathbf{G}} \times_1 \mathbf{A}^{(1)} \times_2 \mathbf{A}^{(2)} \times_3 \mathbf{A}^{(3)} = \underline{\mathbf{X}} \times_4 \left(\mathbf{A}^{(4)} \right)^{\dagger} \tag{2}$$

$\underline{\mathbf{S}} \in \mathbb{R}_{0^+}^{I_1 \times I_2 \times I_3 \times J}$ contains 3D intensity distributions of the J sources (organs or tissues) present in the image $\underline{\mathbf{X}}$. The '†' symbol in (2) denotes the Moore-Penrose pseudoinverse. Interpretation of the mode-4 matrix $\mathbf{A}^{(4)}$ in (1) and (2) depends on the imaging modality at consideration. In multi-phase CT imaging its column vectors represent density profiles of the organs. In multispectral imaging its column vectors represent spectral profiles of the tissues. We can unfold or matricize tensor (1) along any mode. Mode-4 unfolding yields:

$$\mathbf{X}_{(4)} \approx \mathbf{A}^{(4)} \mathbf{G}_{(4)} \left[\mathbf{A}^{(3)} \otimes \mathbf{A}^{(2)} \otimes \mathbf{A}^{(1)} \right]^{\mathrm{T}} = \mathbf{A}^{(4)} \mathbf{S}_{(4)} \tag{3}$$

where $\mathbf{X}_{(4)} \in \mathbb{R}_{0+}^{I_4 \times I_1 I_2 I_3}$ stands for mode-4 unfolded image tensor $\underline{\mathbf{X}}$, $\mathbf{G}_{(4)} \in \mathbb{R}_{0+}^{J \times J^3}$ stands for mode-4 unfolded core tensor $\underline{\mathbf{G}}$, $\mathbf{S}_{(4)} \in \mathbb{R}_{0+}^{J \times I_1 I_2 I_3}$ stands for mode-4 unfolded source tensor $\underline{\mathbf{S}}$ and $\otimes$ stands for Kronecker's product. It is important to notice that, from the perspective of the matrix factorization method proposed herein, mapping $\underline{\mathbf{X}} \rightarrow \mathbf{X}_{(4)}$ is arbitrary as long as it is used consistently in tensorisation of the factorization results implied by (3), i.e. $\mathbf{S}_{(4)} \rightarrow \underline{\mathbf{S}}$. Eq.(3) is structurally similar to bLMM in instantaneous linear BSS commonly used in unsupervised multichannel image segmentation on a slice-by-slice basis. However, fundamental difference is that in the later case each slice $\left\{ \underline{\mathbf{X}}_{i_3} \in R_{0+}^{I_1 \times I_2 \times I_4} \right\}_{i_3=1}^{I_3}$ is, after mode-3 unfolding, represented by a bLMM:

$$\mathbf{X}_{i_3(3)} \approx \mathbf{A}_{i_3}^{(3)} \mathbf{G}_{i_3(3)} \left[\mathbf{A}_{i_3}^{(2)} \otimes \mathbf{A}_{i_3}^{(1)} \right]^{\mathrm{T}} = \mathbf{A}_{i_3}^{(3)} \mathbf{S}_{i_3(3)} \quad \forall i_3 = 1, \ldots, I_3 \tag{4}$$

where $\mathbf{X}_{i_3(3)} \in \mathbb{R}_{0+}^{I_4 \times I_1 I_2}$ is unfolded slice tensor $\underline{\mathbf{X}}_{i_3}$, $\mathbf{G}_{i_3(3)} \in \mathbb{R}_{0+}^{J \times J^2}$ is mode-3 unfolded core tensor of the related Tucker3 tensor model of the slice tensor $\underline{\mathbf{X}}_{i_3}$, $\left\{\mathbf{A}_{i_3}^{(n)} \in \mathbb{R}_{0+}^{I_n \times J}\right\}_{n=1}^{3}$ are factors of the same Tucker3 model and $\mathbf{S}_{i_3(3)}$ is mode-3 unfolded source tensor $\underline{\mathbf{S}}_{i_3}$. Hence, 3D intensity distributions of the J sources present in the image $\underline{\mathbf{X}}$ can be obtained either by NMF of $\mathbf{X}_{(4)}$ in (3) or by $\left\{\mathbf{X}_{i_3(3)}\right\}_{i_3=1}^{I_3}$ matrices in (4). The former case yields unfolded version $\mathbf{S}_{(4)}$ of the source tensor $\underline{\mathbf{S}}$ and, thus, solves 3D segmentation problem. The last case yields unfolded versions $\left\{\mathbf{S}_{i_3(3)}\right\}_{i_3=1}^{I_3}$ of the source tensors $\left\{\underline{\mathbf{S}}_{i_3}\right\}_{i_3=1}^{I_3}$ and, thus, solves 2D segmentation problems on a slice-by-slice basis. However, while in (3) one mixing matrix, that is $\mathbf{A}^{(4)}$, is common for all the slices 1 to I_3, in (4) each slice is characterized by its own mixing matrix $\left\{\mathbf{A}_{i_3}^{(3)}\right\}_{i_3=1}^{I_3}$. This suggests that 3D segmentation can be more accurate due to the fact that specific source (organ or tissue) is forced to retain the same profile across all the slices. The BSS problem (3), resp. (4), is ill-posed due to the fact that matrix factorization implied by it suffers from indeterminacies: $\mathbf{X}_{(4)} = \mathbf{A}^{(4)}\mathbf{S}_{(4)} = \mathbf{A}^{(4)}\mathbf{B}^{-1}\mathbf{B}\mathbf{S}_{(4)}$ for some square invertible matrix $\mathbf{B}$. Hence, (3) has an infinite number of possible solutions. Meaningful solutions are characterized by the permutation and scaling indeterminacies in which case $\mathbf{B}=\mathbf{P}\mathbf{\Lambda}$, where $\mathbf{P}$ represents permutation and $\mathbf{\Lambda}$ represents diagonal scaling matrix. Constraints are necessary to be imposed on $\mathbf{A}^{(4)}$ and/or $\mathbf{S}_{(4)}$ to obtain solution of (3), resp. (4), unique up to permutation and scaling indeterminacies. To this end, sparseness constraint is imposed on $\mathbf{S}_{(4)}$ in (3), resp. $\left\{\mathbf{S}_{i_3(3):}\right\}_{i_3=1}^{I_3}$ in (4). It is justified by an assumption that only small number (possibly even one) source is dominantly present at each location in the image i.e. $\left\{\underline{\mathbf{X}}_{i_1,i_2,i_3,:}\right\}_{i_1,i_2,i_3=1}^{I_1,I_2,I_3}$.

3 SPARSENESS CONSTRAINED NMF

Sparseness constrained NMF algorithms infer $\mathbf{A}^{(4)}$ and $\mathbf{S}_{(4)}$ from $\mathbf{X}_{(4)}$ in (3) by minimizing difference between data $\mathbf{X}_{(4)}$ and model $\mathbf{A}^{(4)}\mathbf{S}_{(4)}$ such that sparseness constrained is imposed on $\mathbf{S}_{(4)}$. This is usually achieved through alternating least square (ALS) methodology [7, 8]. The local or hierarchical ALS-based NMF, the HALS NMF, algorithm [8] is capable of solving underdetermined BSS problem (4) such that the number of organs J present in the image $\mathbf{X}_{(4)}$ is allowed to be greater than number of measurements (physical channels) I_4. This capability is of great practical importance for low-dimensional imaging modalities such as MR or CT where number of channels is small (3 or 4) and number of organs or tissue types can be up to10. The HALS NMF method has been demonstrated previously for sparseness constrained unsupervised decomposition of RGB image in [9]. The algorithm minimizes global cost function to estimate the mixing matrix $\mathbf{A}^{(4)}$:

$$D\left(\mathbf{X}_{(4)} \middle\| \mathbf{A}^{(4)}\mathbf{S}_{(4)}\right) = \frac{1}{2}\left\|\mathbf{X}_{(4)} - \mathbf{A}^{(4)}\mathbf{S}_{(4)}\right\|_F^2$$

and set of local cost functions to estimate intensity distributions of the tissues $\left\{\mathbf{s}_{j:}\right\}_{j=1}^{J}$, i.e. row vectors of $\mathbf{S}_{(4)}$:

$$D^{(j)}\left(\mathbf{X}_{(4)}^{j} \middle\| \mathbf{a}_{:j}\mathbf{s}_{j:}\right) = \frac{1}{2}\left\|\mathbf{X}_{(4)}^{j} - \mathbf{a}_{:j}\mathbf{s}_{j:}\right\|_F^2 + \alpha_{\mathbf{s}}^{j} J_{\mathbf{S}}(\mathbf{s}_{j:}) \quad \forall j = 1,\ldots,J.$$

Here $\left\{\mathbf{a}_{:j}\right\}_{j=1}^{J}$ represent columns of $\mathbf{A}^{(4)}$, $\mathbf{X}_{(4)}^{j} = \mathbf{X}_{(4)} - \sum_{i \neq j}\mathbf{a}_{:i}\mathbf{s}_{i:}$, $J_{\mathbf{S}}(\mathbf{s}_{j:}) = \sum_{i_1,i_2,i_3=1}^{I_1,I_2,I_3} s_{j(i_1 i_2 i_3)}$ represents sparseness constraint (the ℓ_1-norm of $\mathbf{s}_{j:}$), whereat $\alpha_{\mathbf{s}}^{j}$ stands for regularization constant. Optimal selection of regularization

constants $\left\{\alpha_{\mathbf{s}}^{j}\right\}_{j=1}^{J}$ is what makes the HALS NMF somewhat complicated to apply in truly unsupervised scenarios, i.e. when no ground truth information is available to apply cross-validation and tune the regularization constants $\left\{\alpha_{\mathbf{s}}^{j}\right\}_{j=1}^{J}$. To this end, we have implemented sparseness constrained NMF by nonnegative matrix underapproximation (NMU) algorithm, [10]. In addition to nonnegativity constrains imposed on $\mathbf{A}^{(4)}$ and $\mathbf{S}_{(4)}$, the NMU algorithm minimizes the cost function $D\left(\mathbf{X}_{(4)}\left\|\mathbf{A}^{(4)}\mathbf{S}_{(4)}\right.\right)=\left\|\mathbf{X}_{(4)}-\mathbf{A}^{(4)}\mathbf{S}_{(4)}\right\|_F^2$, by imposing an underapproximation constraint: $\mathbf{A}^{(4)}\mathbf{S}_{(4)} \le \mathbf{X}_{(4)}$. Underapproximation constraint yields more localized parts-based decomposition where different basis elements describe disjoint parts of the input data $\mathbf{X}_{(4)}$. Since multispectral MR image is composed of disjoint parts (intensity distribution of the tissues present in the image), the NMU algorithm represented a logical choice for factorization of (3) to perform 3D segmentation of MR image. According to theorem 1 in [10], it is important property of the NMU algorithm to perform factorization such that $s\left(\mathbf{A}^{(4)}\right)+s\left(\mathbf{S}_{(4)}\right)\ge s\left(\mathbf{X}_{(4)}\right)$, where $s(\mathbf{S}_{(4)})$ measures sparseness of $\mathbf{S}_{(4)}$ defined as: $s(\mathbf{S}_{(4)})$=#zeros($\mathbf{S}_{(4)}$)/($J\times I_1 I_2 I_3$) $\in$ [0,1]. $s(\mathbf{A}^{(4)})$ and $s(\mathbf{X}_{(4)})$ are defined analogously. Hence, NMU yields sparse factorization of $\mathbf{X}_{(4)}$ in (3). The NMU method is implemented through minimization of the Lagrangian $L(\mathbf{A}^{(4)},\mathbf{S}_{(4)},\mathbf{\Lambda})$:

$$L\left(\mathbf{A}^{(4)},\mathbf{S}_{(4)},\mathbf{\Lambda}\right)=\frac{1}{2}\left\|\left(\mathbf{X}_{(4)}-\mathbf{\Lambda}\right)-\mathbf{A}^{(4)}\mathbf{S}_{(4)}\right\|_F^2-\frac{1}{2}\left\|\mathbf{\Lambda}\right\|_F^2$$

where $\mathbf{\Lambda}$ stands for matrix of Lagrange multipliers. Columns of $\mathbf{A}^{(4)}$ and rows of $\mathbf{S}_{(4)}$ are alternatively estimated one at a time by means of the HALS NMF algorithm [8], minimizing $\left\|\left(\mathbf{X}_{(4)}-\mathbf{\Lambda}\right)-\mathbf{A}^{(4)}\mathbf{S}_{(4)}\right\|_F^2$, whereat no sparseness constraint are imposed on $\mathbf{S}_{(4)}$. Matrix of Lagrange multipliers is updated as: $\mathbf{\Lambda}\leftarrow\max\left(0,\mathbf{\Lambda}-1/k\left(\mathbf{X}_{(4)}-\mathbf{A}_{(4)}\mathbf{S}^{(4)}\right)\right)$. Unlike HALS NMF method, there are no regularization constants associated with the NMU algorithm. Like HALS NMF algorithm, the NMU algorithm is also capable to solve underdetermined BSS problems. The MATLAB code for the NMU algorithm can be downloaded from [11]. The update rules of the NMU algorithm are summarized below:

1. column-wise update of $\mathbf{A}_{(4)}$: $\mathbf{a}_{:j}=\max\left(0,\frac{\mathbf{c}_{:j}-\sum_{l=1,l\ne j}^{J}\mathbf{a}_{:j}d_{lj}}{d_{jj}}\right)\ \forall j=1,\ldots,J$

   where $\mathbf{C}=\left(\mathbf{X}_{(4)}-\mathbf{\Lambda}\right)\mathbf{S}_{(4)}^{T}$ and $\mathbf{D}=\mathbf{S}_{(4)}\mathbf{S}_{(4)}^{T}$.

2. row-wise update of $\mathbf{S}_{(4)}$: $\mathbf{s}_{j:}=\max\left(0,\frac{\mathbf{e}_{j:}-\sum_{l=1,l\ne j}^{J}f_{jl}\mathbf{s}_{l:}}{f_{jj}}\right)\ \forall j=1,\ldots,J$

   where $\mathbf{E}=\mathbf{A}^{(4)T}\left(\mathbf{X}_{(4)}-\mathbf{\Lambda}\right)$ and $\mathbf{F}=\mathbf{A}^{(4)T}\mathbf{A}^{(4)}$.

3. update of the matrix of Lagrange multipliers $\mathbf{\Lambda}$: $\mathbf{\Lambda}\leftarrow\max\left(0,\mathbf{\Lambda}-\frac{1}{k}\left(\mathbf{X}_{(4)}-\mathbf{A}^{(4)}\mathbf{S}_{(4)}\right)\right)$

   where k stands for iteration index.

4 RESULTS

We demonstrate proposed 3D segmentation method on extraction of brain tumor from synthetic mMR image. The image is obtained from TumorSim database of the Utah Center for Neuroimage Analysis, [5]. In relation to standard mMR image comprised of T1, T2 and PD images, the PD image has been replaced by T1-weighted image obtained after administration gadolinium contrast agent. We have applied proposed 3D segmentation method to slices 50 to 70 of the TumoSimData_004 dataset. Thus, I_3=21 slices were segmented jointly. Each slice has 256×256 pixels. Thus the image tensor was of the size $\underline{\mathbf{X}} \in R_{0+}^{256\times256\times21\times3}$. T1, T2 and T1_GAD images for every second slice from 52 to 68 are shown in Figure 1. Figure 2 shows results obtained by proposed 3D segmentation method, while Figure 3 shows corresponding ground truth results. Results of quantitative performance analysis are reported in Table 1 in term of Dice's coefficient. They are compared favorably against those based on T1 weighted image only and that is obtained after administration gadolinium contrast agent. Values of Dice's coefficient are relatively low due to small visible presence of non-tumor tissues in extracted tumor component. This will be improved in future work by using nonlinear version of proposed method in the spirit of nonlinear multispectral image segmentation method presented in [12].

Table 1. Segmentation results in term of Dice's coefficient for slices 50 to 70.

Slice number	*50*	*51*	*52*	*53*	*54*	*55*	*56*	*57*	*58*	*59*	*60*
3D Segmentation	0.532	0.575	0.627	0.637	0.647	0.639	0.600	0.514	0.457	0.423	0.367
T1_GAD image	0.017	0.019	0.021	0.022	0.024	0.024	0.029	0.037	0.044	0.047	0.050
Slice number	*61*	*62*	*63*	*64*	*65*	*66*	*67*	*68*	*69*	*70*	
3D Segmentation	0.427	0.451	0.473	0.480	0.439	0.343	0.359	0.305	0.224	0.218	
T1_GAD image	0.052	0.054	0.055	0.057	0.059	0.060	0.061	0.061	0.061	0.060	

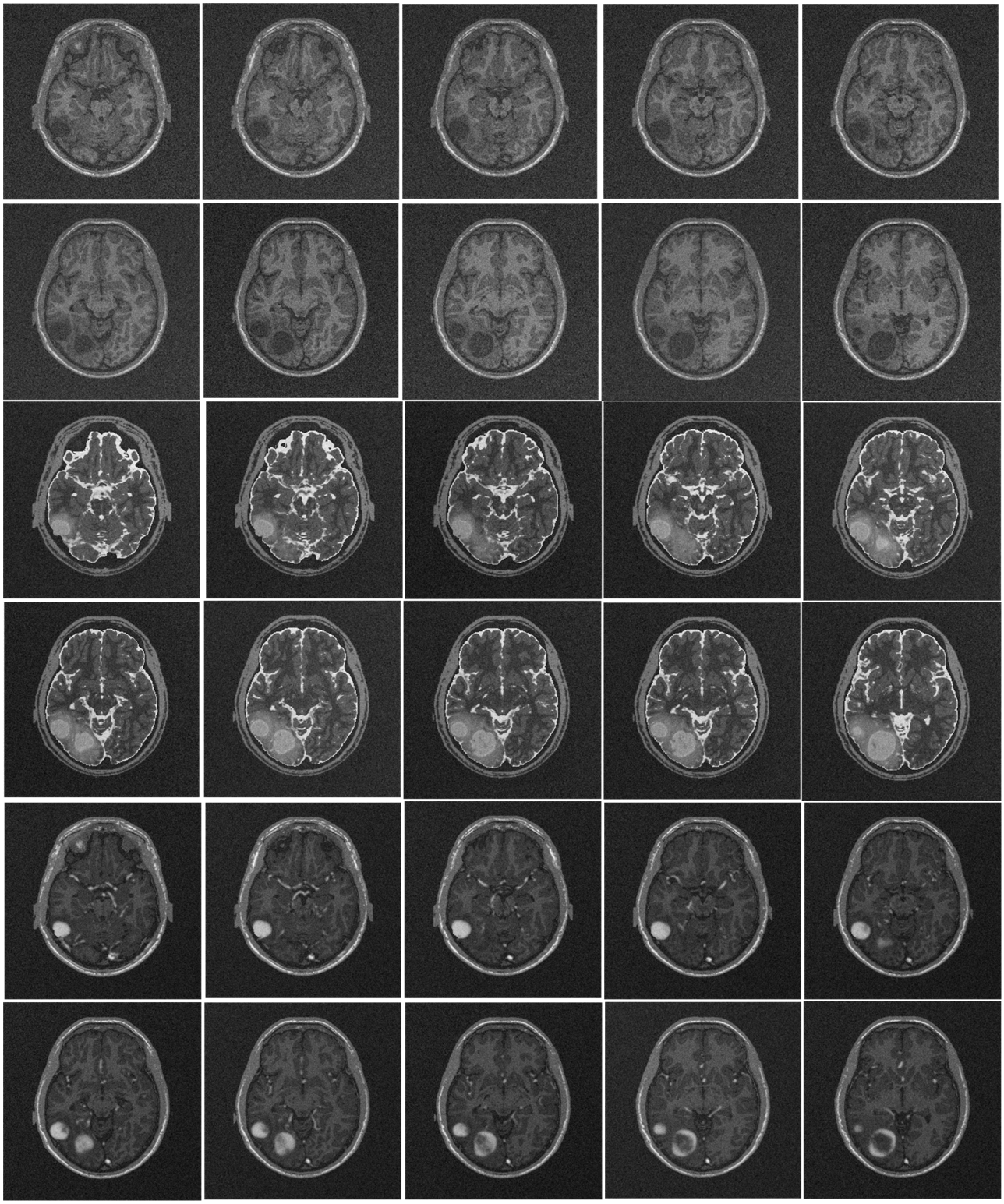

Figure 1. Every second slice from 52 to 70 of mMR of the brain with a tumor: T1 image (top two rows), T2 image (third and fourth row) and T1_GAD image (last two rows).

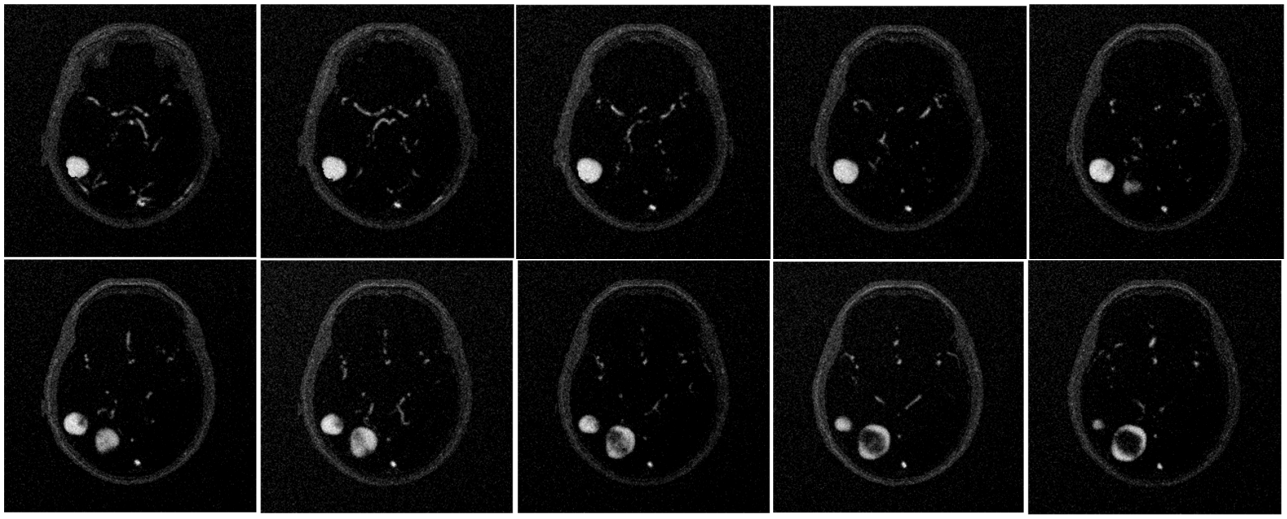

Figure 2. Results of proposed 3D segmentation method for every second slice from 52 to 70.

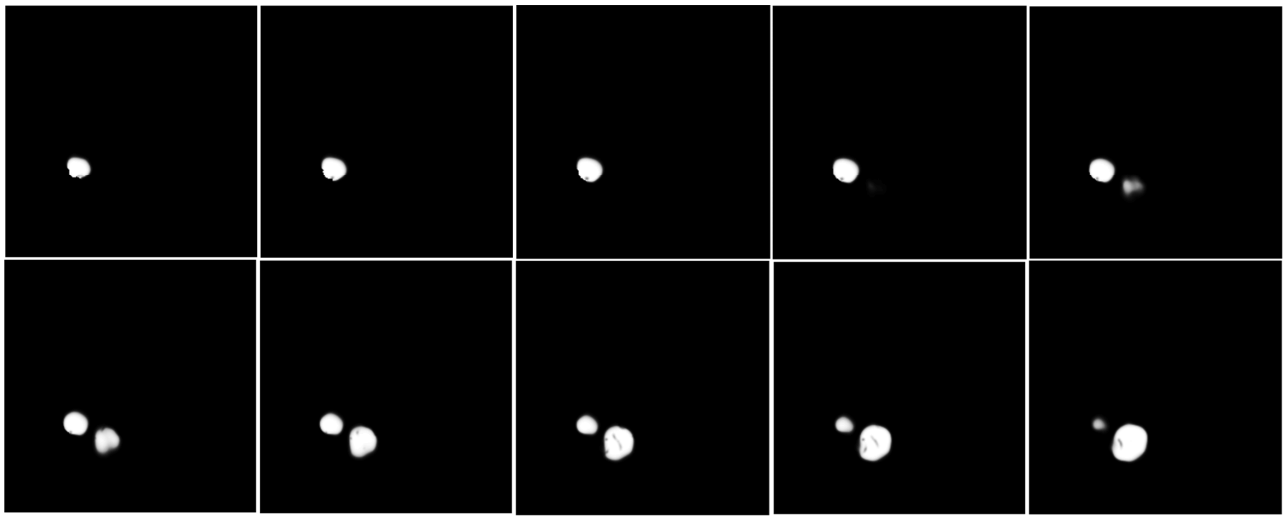

Figure 3. Tumor ground truth for every second slice from 52 to 70.

5 CONCLUSION

Methodology for unsupervised 3D segmentation of organs (tissues) from registered multichannel images is proposed. The methodology treats the multislice multichannel image as 4D tensor that is represented by multilinear mixture model, i.e. the image is modeled by a weighted linear combination of 3D intensities of the objects present in the image. 3D segmentation problem is solved by sparseness constrained factorization of nonnegative matrix obtained by mode-4 unfolding of the 4D image tensor. Proposed method is preliminary demonstrated on extraction of brain tumor from synthetic mMR image. It is however understood that it can be applied to 3D segmentation of organs or tissues from images acquired by different multichannel medical imaging modalities such as multi-phase CT, multispectral/hyperspectral, diffusion tensor and/or optical coherence tomography images.

ACKNOWLEDGEMENTS

The work of I. Kopriva and A. Jukić has been supported through grant 098-0982903-2558 funded by the Ministry of Science, Education and Sports, Republic of Croatia.

REFERENCES

[1] Kopriva, I., Chen, X., and Jao, Y. "Nonlinear Band Expansion and Nonnegative Matrix Underapproximation for Unsupervised Segmentation of a Liver from a Multi-phase CT image," Proc. SPIE Vol. 7962,79623A-1-79623A-8, 2011.

[2] Kopriva, I., and Cichocki, A. "Nonlinear Band Expansion and 3D Nonnegative Tensor Factorization for Blind Decomposition of Magnetic Resonance Image of the Brain," Lecture Notes Computer Science 6365, 490-497, 2010.

[3] Hyvärinen, A., Karhunen, J., and Oja, E., [Independent Component Analysis], Wiley Interscience (2001).

[4] Cichocki, A., and Amari, S. I., [Adaptive Blind Signal and Image Processing], John Wiley (2002).

[5] The TumorSim database of Utah Center for Neuroimage Analysis: http://www.nitrc.org/projects/tumorsim/.

[6] Tucker, L. R., "Some mathematical notes on three-mode factor analysis," Psychometrika 31, 279-311 (1966).

[7] Cichocki, A., Zdunek, R., Phan, A. H., and Amari, S. I., [Nonnegative Matrix and Tensor Factorization], John Wiley & Sons (2009).

[8] Cichocki A., Zdunek R., and Amari S. I. Hierarchical ALS Algorithms for Nonnegative Matrix Factorization and 3D Tensor Factorization. Lecture Notes Computer Science 4666, 169-176, 2007.

[9] Kopriva, I., and Cichocki, A. "Blind decomposition of low-dimensional multi-spectral image by sparse component analysis," Journal of Chemometrics 23, 590-597 (2009).

[10] Gillis, N., and Glineur, F. "Using underapproximations for sparse nonnegative matrix factorization," Pattern Recognition 43, 1676-1687 (2010).

[11] MATLAB code of the NMU algorithm: https://sites.google.com/site/nicolasgillis/code

[12] Kopriva, I., Hadžija, M., Popović-Hadžija, M., Korolija, M., and Cichocki, A., "Rational Variety Mapping for Contrast-Enhanced Nonlinear Unsupervised Segmentation of Multispectral Images of Unstained Specimen," The American Journal of Pathology 179, 547-553 (2011).